Global Change Biology

Global Change Biology (2016) **22**, 644–655, doi: 10.1111/gcb.13081

Temperature, precipitation, and insolation effects on autumn vegetation phenology in temperate China

QIANG LIU[1], YONGSHUO H. FU[1,2], ZHENZHONG ZENG[1], MENGTIAN HUANG[1], XIRAN LI[1] and SHILONG PIAO[1,3]

[1]*Sino-French Institute for Earth System Science, College of Urban and Environmental Sciences, Peking University, Beijing 100871, China,* [2]*Centre of Excellence PLECO (Plant and Vegetation Ecology), Department of Biology, University of Antwerp, Universiteitsplein 1, B-2610 Wilrijk, Belgium,* [3]*Institute of Tibetan Plateau Research, Center for Excellence in Tibetan Earth Science, Chinese Academy of Sciences, Beijing 100085, China*

Abstract

Autumn phenology plays a critical role in regulating climate–biosphere interactions. However, the climatic drivers of autumn phenology remain unclear. In this study, we applied four methods to estimate the date of the end of the growing season (EOS) across China's temperate biomes based on a 30-year normalized difference vegetation index (NDVI) dataset from Global Inventory Modeling and Mapping Studies (GIMMS). We investigated the relationships of EOS with temperature, precipitation sum, and insolation sum over the preseason periods by computing temporal partial correlation coefficients. The results showed that the EOS date was delayed in temperate China by an average rate at 0.12 ± 0.01 days per year over the time period of 1982–2011. EOS of dry grassland in Inner Mongolia was advanced. Temporal trends of EOS determined across the four methods were similar in sign, but different in magnitude. Consistent with previous studies, we observed positive correlations between temperature and EOS. Interestingly, the sum of precipitation and insolation during the preseason was also associated with EOS, but their effects were biome dependent. For the forest biomes, except for evergreen needle-leaf forests, the EOS dates were positively associated with insolation sum over the preseason, whereas for dry grassland, the precipitation over the preseason was more dominant. Our results confirmed the importance of temperature on phenological processes in autumn, and further suggested that both precipitation and insolation should be considered to improve the performance of autumn phenology models.

Keywords: autumn phenology, China, climate change, end of growing season, insolation, normalized difference vegetation index

Received 12 August 2015; revised version received 12 August 2015 and accepted 20 August 2015

Introduction

Climate change affects the ecosystems regionally and globally (Visser & Both, 2005; Piao *et al*., 2007, 2009; Richardson *et al*., 2013; Hilker *et al*., 2014; Piao *et al*., 2015; Brandt *et al*., 2015). Numerous studies based on both ground and satellite observations have reported a progressively earlier start of vegetation growing season (SOS) during spring (Schwartz *et al*., 2006; Fu *et al*., 2014a; Wang *et al*., 2015) and a less consistent end of vegetation growing season (EOS) in autumn (Menzel & Fabian, 1999; Jeong *et al*., 2011; Yang *et al*., 2014). Compared with SOS (Cleland *et al*., 2007; Yu *et al*., 2010; Guo *et al*., 2015), the response of EOS to climate change has drawn less attention (Miloud & Ali, 2012; Gallinat *et al*., 2015). Recent studies revealed that EOS may even contribute larger than SOS in the extension of growing season length (Zhu *et al*., 2012; Garonna *et al*., 2014) and hence play a fundamental role in regulating the carbon balance in temperate vegetation (Piao *et al*., 2008; Richardson *et al*., 2009). However, the phenological processes of plants in autumn are complex (Gan & Amasino, 1997; Estiarte & Peñuelas, 2015). Therefore, investigation of EOS variation and corresponding climatic drivers is essential to improve autumn phenology models and to enrich our understanding of the responses of the carbon cycle to ongoing global climate changes.

In situ records could provide accurate phenological information at the species level, but they are limited in their spatial scope (Cleland *et al*., 2007; Studer *et al*., 2007). Remote sensing-based land surface phenology provides large-scale observations and has been used frequently in recent years (Stöckli & Vidale, 2004; White *et al*., 2009). Different methods have been proposed to retrieve EOS date from satellite records. These methods generally consist of two main steps, that is, elimination of noise from NDVI curve and determination of the EOS date. In the first step, lots of smoothing functions,

Correspondence: Shilong Piao, tel. +86 10 6276 5578, fax +86 10 6275 6560, e-mail: slpiao@pku.edu.cn

such as HANTS (Roerink *et al*., 2000; Cong *et al*., 2012), wavelet (Sakamoto *et al*., 2005), Fourier analysis (Moody & Johnson, 2001), and S-G filtering (Chen *et al*., 2004), have been introduced to reduce the influence of noise. In the second step, various criteria have been applied, mainly in two sorts: first, thresholds based on predefined value (Myneni *et al*., 1997; Zhou *et al*., 2003; Delbart *et al*., 2005; Philippon *et al*., 2007) or maximum change of NDVI data (Moulin *et al*., 1997; Piao *et al*., 2006; Balzter *et al*., 2007), and second, changing characteristics in temporal NDVI profile, such as inflection point (Julien & Sobrino, 2009) and maximum of rate of change of curvature (Tucker *et al*., 2001; Zhang *et al*., 2003; Shen *et al*., 2015). Whereas these methods differ in their interpretation of phenological metrics from time-series NDVI data (White *et al*., 2009), caution is therefore warranted when discussing EOS variation based on a single method. A combination of multiple methods is thus needed to capture variation in EOS over time and to assess relationships with climatic factors.

The vast territory, complex terrain, and rich biodiversity in China make it a reasonable choice for investigation on the response of phenological events to climate change. Preceding studies in this region mainly focused on the exploration of SOS (Piao *et al*., 2011; Cong *et al*., 2013; Wu & Liu, 2013; Ge *et al*., 2014), few of them, however, discussed the variation of EOS, especially their relationship with climatic factors. Piao *et al*. (2006) and Yang *et al*. (2014) conducted their researches on the change of EOS in China and Che *et al*. (2014) focused on Qinghai–Tibet Plateau, but all of them were implemented by single approach. Moreover, these studies attempted to explain the variation of EOS through temperature and precipitation, while neglected the role of light conditions in triggering EOS, such as photoperiod and/or light intensity (Keskitalo *et al*., 2005; Günter *et al*., 2008; Jeong & Medvigy, 2014; Borchert *et al*., 2015). In regional investigations of the light influence, solar radiation could be used as a combination of both photoperiod and solar intensity (Calle *et al*., 2010). Therefore, total received daily shortwave downward radiation (referred to insolation sum) should be included to further discuss the climatic control on EOS.

In this study, we investigated variation in EOS over the period 1982–2011 in temperate China using Global Inventory Modeling and Mapping Studies (GIMMS) normalized difference vegetation index (NDVI) records based on four widely used methods. We applied partial correlation analysis to determine the relationship of EOS with temperature, precipitation, and insolation. The objectives of this research were to (i) quantify trends in EOS across different vegetation types in temperate China and (ii) explore the relationships of EOS with temperature, precipitation, and insolation.

Materials and methods

Study area and biomes

Our study focused on temperate China (70–140°E and 30–55°N). This region was selected for the clear seasonality of natural vegetation, and the satellite NDVI data (i.e., GIMMS $NDVI_{3g}$ datasets) are least impacted by solar zenith angle effects at mid- to high latitudes (Slayback *et al*., 2003; Piao *et al*., 2006). Eight temperate biomes were identified through the rasterization of a digitized 1 : 1 000 000 vegetation map of China (Fig. S1). Pixels dominated by cropland were excluded from our study because its seasonal variability can be easily influenced by human intervention. To reduce the influence of noise and non-vegetation signals on the NDVI time series, we extracted pixels with mean annual NDVI (from 1982 to 2011) greater than 0.1, as lower values usually indicate bare soil or sparse vegetation (Zhou *et al*., 2001; Jeong *et al*., 2011).

Datasets

NDVI and climate datasets. We used the latest release of NDVI data from the Advanced Very High Resolution Radiometer (AVHRR), which is the third-generation dataset (commonly referred to $NDVI_{3g}$) and provided by NASA's GIMMS group (Tucker *et al*., 2004, 2005). In this version, errors and noises resulted from orbital drift, calibration, viewing geometry, stratospheric volcanic aerosols, and other factors unrelated to vegetation dynamics have been reduced (Vermote *et al*., 1997; Pinzon *et al*., 2005; Sobrino *et al*., 2008; Pinzon & Tucker, 2014). This version contains over 30 years of observations of fortnightly maximum value compositions (MVC) at a spatial resolution of one-twelfth of a degree (~ 8 km). To produce the time-series NDVI curve and derive EOS, we extracted pixels covering complete years (from January 1982 to December 2011) and set the middle of the whole compositing period as the acquisition date of each NDVI image. Consistent with NDVI data time period, the gridded daily air temperature, precipitation, and insolation data, with spatial resolution of 0.1° × 0.1°, were extracted from the China Meteorological Forcing Dataset (Yang *et al*., 2006, 2010; Chen *et al*., 2011).

Estimation of EOS

The chlorophyll in plant leaves could strongly absorb red light for the purpose of photosynthesis and reflect near-infrared light. Snow exhibits divergent spectral response pattern to plant. When the surface is covered with snow, the detected NDVI value is quite lower and would misrepresent the photosynthetic capacity of plant. In addition, phenology extraction methods (e.g., piecewise logistic and double logistic) are usually sensitive to the value on the both sides of NDVI curve (non-growing season), which is likely to be affected by snow coverage. Therefore, the influence of snow covered NDVI should be eliminated first (Shen *et al*., 2013). Due to the absence of snow information in GIMMS $NDVI_{3g}$ dataset, we

applied daily air temperature to help identify pixels probably covered by snow (below 0 °C for a sequence of 5 days), replace them with nearest valid NDVI (i.e., snow-free), and restrict the derived EOS within the thermal growing season. This methodology has also been applied by previous studies (Zhang *et al*., 2006; Tan *et al*., 2011). Subsequently, a five-point median-value moving average method was applied to distinguish the abnormal high/low points resulting from residual noise. These points were replaced by corresponding data from the smoothed curve. Finally, we applied four methods based on thresholds or changing characteristics in temporal NDVI profile to determine EOS of individual years. Details of these methods were described below.

HANTS-Maximum method. The HANTS-Maximum method (HANTS-Mr) employs the harmonic analysis of time series (HANTS), adapted from the fast Fourier transform (FFT) algorithm (Jakubauskas *et al*., 2001; De & Su, 2005), and can be used to fit non-uniformly spaced data. HANTS-Mr discards the least significant frequencies (noise, such as cloud cover and other disturbing effects) presented in the NDVI time profiles, and applies a least squares curve fitting procedure based on low-frequency harmonic components. We calculated the relative change of multiyear averaged NDVI using Eqn (1) and identified the time t of maximum decrease. The corresponding NDVI (t + 1) was regarded as the threshold for the estimation of EOS.

$$\mathrm{NDVI}_{\mathrm{ratio}}(t) = \frac{\mathrm{NDVI}(t+1) - \mathrm{NDVI}(t)}{\mathrm{NDVI}(t)}, \quad (1)$$

Based on the smoothed NDVI seasonal curve using HANTS, the date of EOS in autumn was defined as the day when the smoothed curve passes the NDVI threshold.

Polyfit-Maximum methods. Polyfit-Maximum methods (Polyfit-Mr) were used to apply a polynomial function to fit the phenological records (e.g., NDVI; Piao *et al*., 2006) and then used to identify the date of the growing season transition (e.g., SOS; Jeong *et al*., 2011; Cong *et al*., 2012, 2013). The relative change in multiyear averaged NDVI was calculated using Eqn (1). The minimum $\mathrm{NDVI}_{\mathrm{ratio}}$ at time t and the corresponding threshold NDVI (t + 1) were determined to derive EOS dates from the NDVI time-series data, filtered by the inverted 6-degree (n = 6) parabola equation provided below.

$$\mathrm{NDVI}(t) = \alpha_0 + \alpha_1 t^1 + \alpha_2 t^2 + \ldots + \alpha_6 t^6, \quad (2)$$

where t is the Julian date. Regression coefficients, optimized with the Levenberg–Marquardt (LM) method (Moré, 1978), were applied to transform biweekly GIMMS NDVI data to resolution on a daily basis.

Double logistic method. The double logistic method was initially proposed by Pinty *et al*. (2007) to retrieve land surface phenology [Eqn (3)] and was further developed by Julien & Sobrino (2009) to fit NDVI annual evolution. Eqn (4) was adapted for vegetation with higher chlorophyll activity during the beginning and end of the year. Both formulas were used during the fitting process. The root mean square error (RMSE) between the fitted curve and NDVI data was then applied to identify the best choice.

$$\mathrm{NDVI}(t) = \mathrm{wNDVI} + (\mathrm{mNDVI} - \mathrm{wNDVI}) \times \left(\frac{1}{1+e^{-mS(t-S)}} + \frac{1}{1+e^{mA(t-A)}} - 1\right), \quad (3)$$

$$\mathrm{NDVI}(t) = \mathrm{mNDVI} - (\mathrm{mNDVI} - \mathrm{wNDVI}) \times \left(\frac{1}{1+e^{-mS(t-S)}} + \frac{1}{1+e^{mA(t-A)}} - 1\right), \quad (4)$$

where NDVI(t) is the remotely sensed NDVI for a given year, t is the Julian date varying from 1 to 365, mNDVI is the maximum NDVI value during the entire year, wNDVI is the minimum NDVI value, S is the increasing inflection point (spring date), A is the decreasing inflection point (autumn date), and mS and mA are the change rates at the corresponding inflection points. In our research, we calculated these parameters per pixel and per year from NDVI data using the iterative nonlinear least square technique (i.e., LM method).

Piecewise logistic method. The piecewise logistic method uses pairs of sigmoidal functions (Zhang *et al*., 2003, 2006) to fit the temporal trajectory of NDVI data to individual growth cycles for vegetative growth and senescence. It can be expressed with the combination of two separate logistic curves using the following equation:

$$\mathrm{NDVI}(t) = \begin{cases} \frac{c_1}{1+e^{a_1+b_1 t}} + d_1 & t \le \alpha \\ \frac{c_2}{1+e^{a_2+b_2 t}} + d_2 & t > \alpha \end{cases}, \quad (5)$$

where t is the Julian date of each pixel, α indicates the date that divides the NDVI curve into two separate halves, a_1 (a_2) and b_1 (b_2) are empirical coefficients associated with the timing and change rate in the NDVI curve, the parameter $c_1 + d_1$ ($c_2 + d_2$) represents the maximum NDVI value for a predefined period of vegetative growth, and d_1 (d_2) is the initial background value. All parameters were calculated using the LM methods. Local minima for the derivatives of fitted NDVI curve are then used to determine EOS.

Analysis

We first estimated EOS for each year at each pixel using each of the four methods in temperate China from 1982 to 2011, and then, we calculated the temporal trend using simple linear regression and determined its significance at each pixel. For each method, the mean value, standard deviation, and temporal trends of the EOS dates were determined for each biome. The method ensemble mean value of EOS and its temporal trends were also calculated. Correlation coefficients between EOS and temperature, precipitation, and insolation within different lagged months before EOS were calculated to identify the most related periods of climate factors (Piao *et al*., 2006). The preseason was defined as the periods (with one-month steps) before the EOS date for which the correlation coefficient between EOS and climatic factors was highest during 1982–2011. The preseason for each of the three climatic factors, that is, temperature, precipitation, and insolation, was determined separately. Subsequently, we applied a temporal partial

correlation analysis between EOS and mean temperature, precipitation sum, and insolation sum over the preseason. The ensemble mean of the partial correlation coefficients was calculated for each and across all biomes. This method can explore the linkage between EOS and single climate factor while eliminating the effects of the two remaining climate factors in our study (Peng *et al.*, 2013; Fu *et al.*, 2014b; Piao *et al.*, 2014).

Results

Autumn phenology and its temporal variations

The spatial distribution of EOS date roughly followed latitude and altitude patterns in all four methods (Fig. 1). Early EOS was found at higher latitudes (e.g., northeast China) or altitudes (e.g., Qinghai–Tibet Plateau), whereas the latest EOS was mainly in the southern part of temperate China (Fig. 1). The results based on HANTS-Mr, Polyfit-Mr, and piecewise logistic methods (Fig. 1a, b, d) showed similar patterns, whereas EOS based on double logistic (Fig. 1c) was much earlier. At biome scale (Fig. 2), earlier EOS was observed in deciduous needle-leaf forests (DNF; 272 ± 7) and meadows (279 ± 12). Grassland located in Inner Mongolia (GRA-IM) has a remarkable later EOS (289 ± 7) than that in Qinghai–Tibet Plateau (GRA-QT; 280 ± 8). EOS across biomes in temperate china was significantly different in the one-way ANOVA test ($P < 0.01$, Fig. S2).

From 1982 to 2011, the mean date of EOS in temperate China was delayed by an average of 0.12 ± 0.01 days per year. The trends reported by individual methods were similar (Fig. 3). The delay of EOS was extensively observed across more than 67% of the study area, with

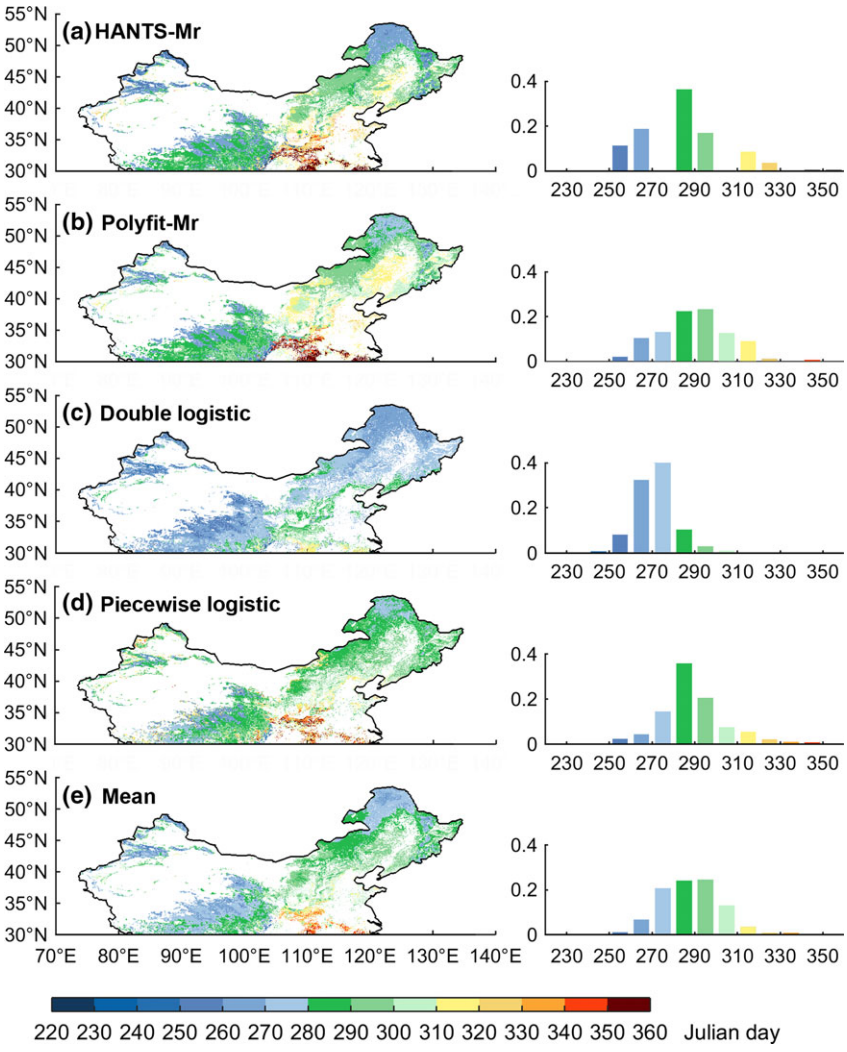

Fig. 1 Spatial patterns of EOS derived from multiyear averaged NDVI data using four methods: HANTS-Mr (a), Polyfit-Mr (b), double logistic (c), piecewise logistic (d), and mean EOS (e). Inset plots (right panels) display the frequency distribution of EOS.

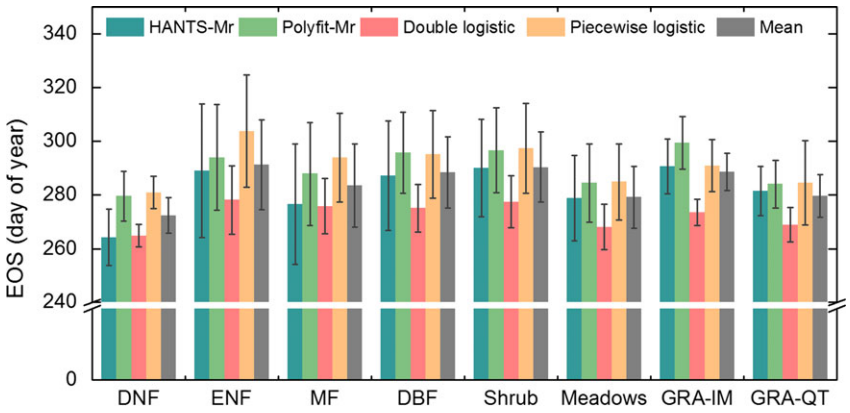

Fig. 2 Average dates and standard deviation of the end of growing season (EOS; day of year) on a biome scale in temperate China for each and all methods, that is, HANTS-Mr, Polyfit-Mr, double logistic, piecewise logistic, and their mean. Eight main biomes in this study area were listed in each columns, such as deciduous needle-leaf forests (DNF), evergreen needle-leaf forests (ENF), mixed forests (MF), deciduous broadleaf forests (DBF), shrub, meadows, and grassland in Inner Mongolia (GRA-IM) and in Qinghai–Tibet Plateau (GRA-QT).

~ 30% of the pixels showing significant delays ($P < 0.05$) (Fig. 3, right panels). However, the northwest of Inner Mongolia, and part of the Qinghai–Tibet Plateau experienced earlier EOS during the same period. In addition, the temporal changes in EOS were biome dependent across the four methods. Significant delayed EOS was observed in most biomes, except for the grassland in Inner Mongolia (GRA-IM), which had an earlier but insignificant EOS trend (-0.02 ± 0.01 days per year). In terms of trends (in days per year) averaged across the four methods, forests, including DNF (0.17 ± 0.03), ENF (0.27 ± 0.05), MF (0.18 ± 0.02), and DBF (0.16 ± 0.01), had a greater delay in EOS than did GRA-QT (0.02 ± 0.01), meadows (0.08 ± 0.01), and shrub (0.14 ± 0.02). Similar results were consistently observed for each of the four methods (Fig. 4).

Correlations between EOS and climatic factors

At the regional scale, EOS in temperate China was correlated with mean temperature during the periods of 1–5 months (both the median and mean occurred at about 3 months) prior to EOS, suggesting that temperature during summer affects EOS dates in autumn (Fig. 5a). With regard to effects of the precipitation and insolation, the periods most associated with EOS were 1–3 and 1–5 months prior to EOS, respectively (Fig. 5a). The preseason lengths were consistent across the four methods for all three climatic factors (Fig. S3a–d).

In general, EOS was positively correlated with both mean temperature and precipitation sum during the preseason (Fig. 5b). Positive partial correlations were observed in more than 67% (temperature) and 62% (precipitation) of the study areas regardless of individual methods (Fig. S3), and ~ 25% of these correlations were statistically significant at $P < 0.05$ (Fig. 5b). In contrast to temperature and precipitation, the partial correlation between EOS and insolation sums during the preseason was quite ambiguous and less apparent as similar proportions of negative and positive partial correlation coefficients were found (Fig. 5b, Fig. S3e–h). Furthermore, the partial correlations of insolation and precipitation with EOS were biome specific.

Biome-specific partial correlations between the mean EOS and climatic factors are provided in Fig. 6. Consistent with the across-biome analysis provided above, a positive partial correlation between EOS and temperature was observed at more than 70% of the pixels of each biome, except for GRA-IM (55%) and meadows (66%), and around 20% of these positive correlations were significant. Consistent results were found in each of the four methods (Fig. S4–7). On the contrary, the partial correlations of EOS with precipitation and insolation sums during the preseason were biome dependent. For the deciduous forests (e.g., DNF and DBF) and the mixed forests (Fig. 6a, c, d), insolation sum was positively associated with EOS, and positive partial correlations were found at more than 70% of the study area, and more than 20% of them were significant. The partial correlation between EOS and precipitation was lower in deciduous and mixed forests. In contrast, for the evergreen needle-leaf forest (Fig. 6b), the precipitation sum was positively associated with EOS for about 64% pixels, and these correlations were significant in about 25% pixels, while the effect of insolation was weak. Interestingly, partial correlations between EOS and insolation for DNF (more than 92%) were positive (Fig. 6a) and were even stronger than correlations between EOS and temperature, suggesting that insolation during

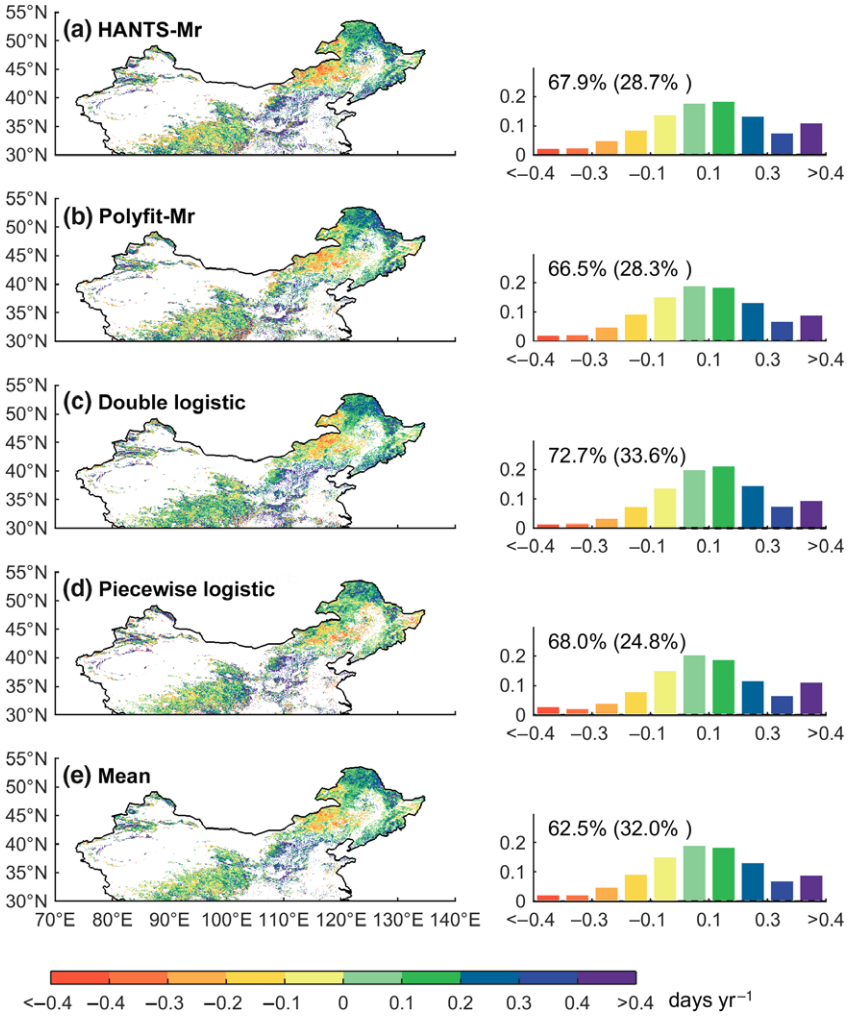

Fig. 3 The spatial distribution of the linear trend of EOS from each and all methods. Fig. 3a–d indicates the change in EOS derived from HANTS-Mr, Polyfit-Mr, double logistic, and piecewise logistic, respectively. Fig. 3e Average of these four methods. The positive value indicates later onset of autumn. Inset plots (right panels) represent the distribution of linear trends for each method. The proportions of positive and significant (in parentheses) trends are provided.

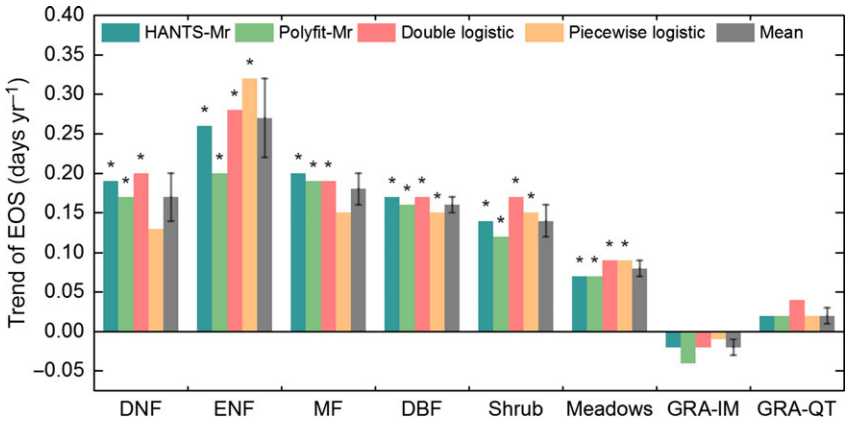

Fig. 4 Linear trends of EOS across China's temperate biomes from 1982 to 2011. The trend in each biome was based on the EOS derived from the averaged NDVI values from all pixels in each biomes. * indicates statistically significant trends at the 95% ($P < 0.05$) level. The average trend and standard deviation were calculated across the four individual methods.

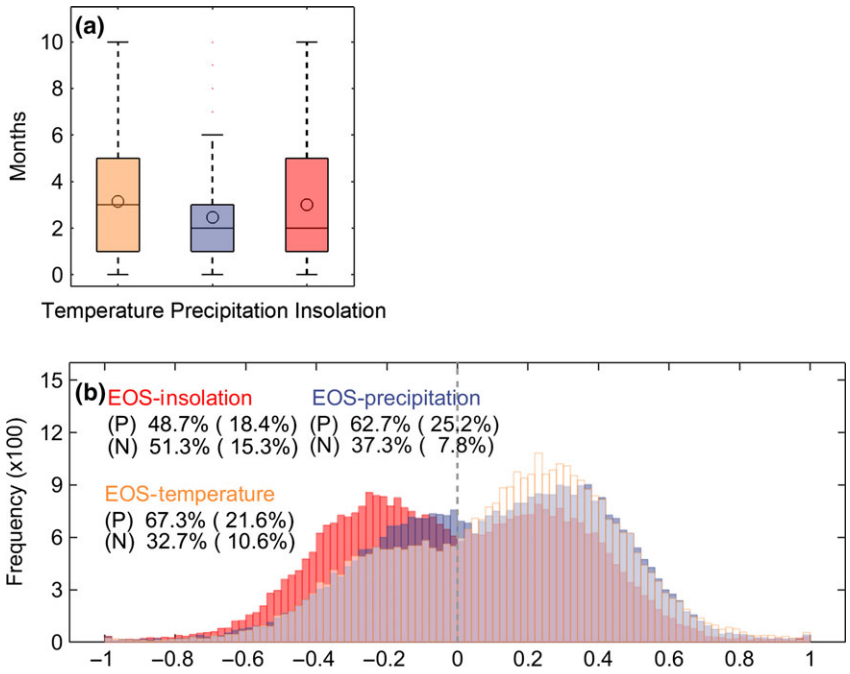

Fig. 5 Preseason durations of climate factors (a) and frequency distributions of partial correlation coefficients between multimethods averaged EOS and climate factors (b). Preseason means the periods preceding the EOS date most related to the variation in EOS. Horizontal lines in each box (Fig. 5a) represent the median values, while open circles indicate mean values. Percentage of positive (P) and negative (N) correlations and corresponding significant correlations ($P < 0.05$, in parentheses) are provided (Fig. 5b).

the preseason may be the dominant determinant of EOS for DNF in temperate China.

With respect to shrub and meadows (Fig. 6e, f), the results revealed positive partial correlations of EOS with precipitation at 68% of shrub (27% were significant) and 60% of meadows' (19% were significant) pixels, respectively. Similar results were found in temperature, with partial correlations in 70% (25% were significant) of shrub and 66% (19% were significant) of meadows' areas. However, the effect of insolation was ambiguous, with only 55% of shrub and 56% of meadows expressed positive correlations (about 15% and 16% of them were significant). These results indicate that both precipitation and temperature during the preseason, rather than insolation, largely determined EOS across these two biomes.

Furthermore, we found substantial differences between grassland in Inner Mongolia (GRA-IM) and that on the Qinghai–Tibet Plateau (GRA-QT) in terms of correlations with climate variables. For the GRA-IM, which is characterized by a dry climate (mean annual precipitation < 400 mm), the partial correlation between the precipitation sum during the preseason was positively correlated with EOS over 84% of the area, and 35% of these relationships were significant; this relationship was much stronger than those for temperature and insolation (Fig. 6g). In contrast, GRA-QT, distributed in the highest plateau in the world (with mean annual temperature below 0 °C), the partial correlation between temperature and EOS (positive in 70% of the study area, with those correlations being significant in about 20%) was greater than those for precipitation and insolation. This suggests that precipitation was a dominant determinant of EOS in dry grasslands but that temperature primarily controlled the grassland EOS in cold regions. This finding was consistent across the four methods (Fig. S4–7).

Discussion

Relationship between EOS and climatic factors

Consistent with previous studies (Estrella & Menzel, 2006; Delpierre *et al.*, 2009; Vitasse *et al.*, 2009; Ge *et al.*, 2014; Yang *et al.*, 2014), we found that warmer summer and autumn led to delayed EOS across vegetation in temperate China. The positive partial correlation between preseason temperature and EOS may be partly due to the fact that higher temperatures in the summer and autumn could enhance activities of photosynthetic enzymes (Shi *et al.*, 2014) and slow the speed of chlorophyll degradation during autumn leaf senescence (Fracheboud *et al.*, 2009). Another possible explanation is that the warmer autumn reduced potential for frost damage due to the reduced

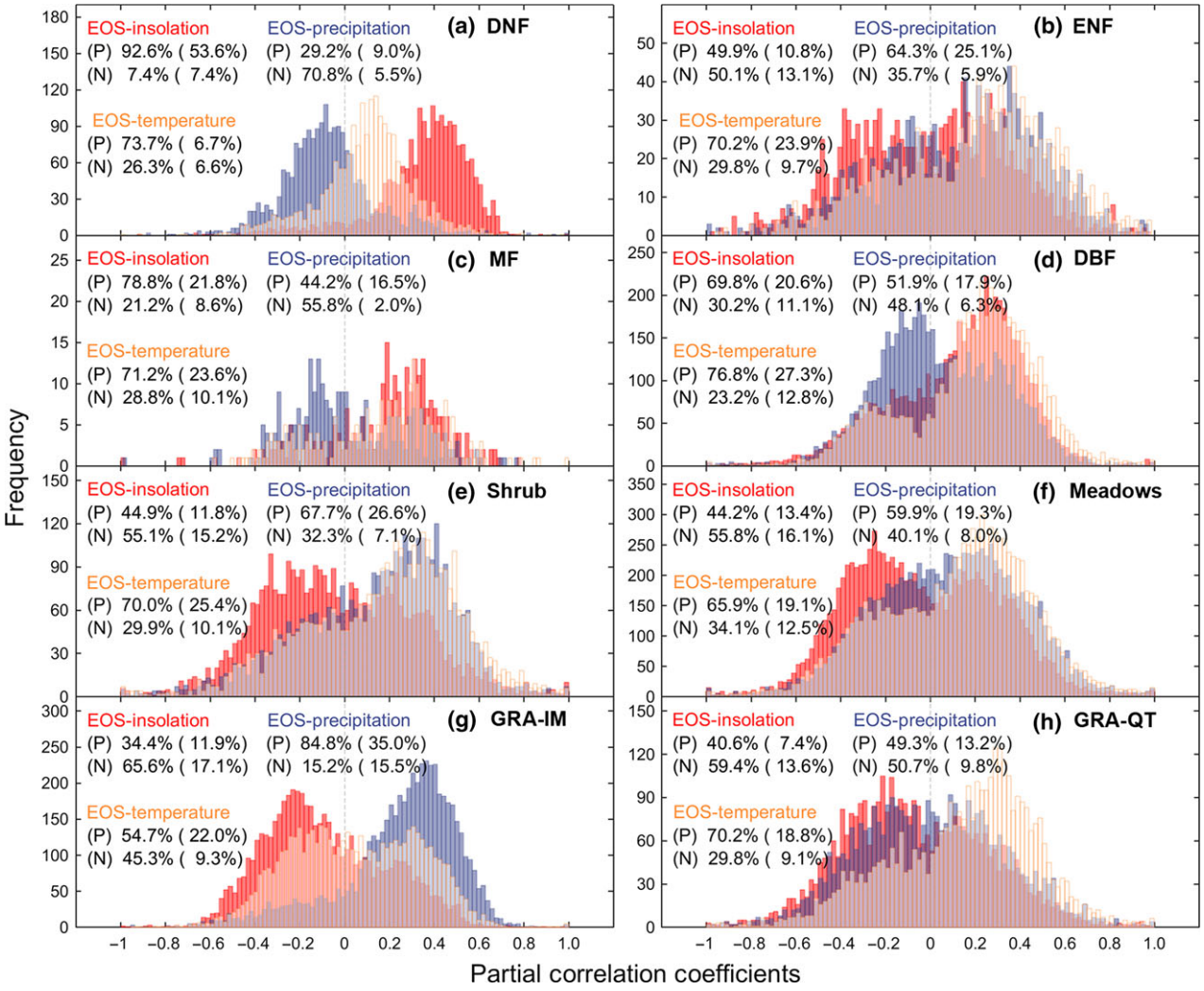

Fig. 6 The frequency distribution of partial correlation coefficients between EOS (averaged from four methods) and climate factors for each biomes in temperate China. Figure 6g (GRA-IM) and Fig. 6h (GRA-QT) represent the grassland located in Inner Mongolia and Qinghai–Tibet Plateau, respectively. The texts in the upper left corner of each subfigure present the percentage of positive (P) and negative (N) correlations ($P < 0.05$, percentage of significant correlations in parentheses) corresponding to preseason temperature mean, precipitation sum, and insolation sum.

number of freezing days (Hartmann *et al*., 2013) and later appearance of first frost day in autumn (Schwartz, 2003).

Additionally, our results revealed positive effects of total preseason precipitation on grassland EOS, especially in dry climate areas, where the effect of precipitation is even larger than that of temperature (e.g., GRA-IM; Fig. 6, Fig. S4–7). These positive correlations might be related to the effect of water stress on plant growth during autumn. Limited water potential would inhibit plant growth and photosynthesis activities (Tezara *et al*., 1999), increase the risk of chlorophyll degradation and plant mortality, and advance the timing of leaf senescence (Munné-Bosch & Alegre, 2004; Anderegg *et al*., 2013; Dreesen *et al*., 2014). Thus, increased precipitation during the preseason period may alleviate water stress and extend the growing season in autumn. However, we did not find these correlations in forest biomes, such as DNF, MF, and DBF, although we did observe them for ENF (Fig. 6, Fig. S4–7), which may be related to relatively higher mean annual precipitation (ranging from ~ 493 mm in DNF to 717 mm in ENF).

Interestingly, we found that, in addition to temperature, insolation was also positively associated with EOS for temperate forests (e.g., DNF, MF, DBF) in China, but weakly correlated with nonforest biomes (e.g., shrub, meadows, GRA-IM, and GRA-QT; Fig. 6, Fig. S4–7), suggesting that light conditions may co-control the date of EOS in temperate forests (Fig. 6a, c, d, Fig. S4–7), especially in DNF, where insolation may play a more dominant role in EOS. The EOS of nonforest biomes

might be more vulnerable to the change of precipitation and/or temperature (see above), while the mechanism by which light controls EOS in forests is still unclear (Biswal & Biswal, 1984; Estiarte & Peñuelas, 2015; Gallinat *et al*., 2015). We investigated the effect of insolation on autumn phenology. Because of the difficulty to disentangle the effects of photoperiod (i.e., day length) and light intensity (Calle *et al*., 2010). We, therefore, investigated the effect of insolation on autumn phenology, and positive influence of insolation on forest EOS was apparent. We proposed three nonexclusive hypotheses to explain the positive correlation between insolation sum over the preseason and EOS for temperate forests in China.

First, the effect of insolation in delaying leaf senescence may be related to its influence on the stomata aperture. Higher insolation in the daytime can retard the accumulation of abscisic acid and subsequently slow the speed of leaf senescence (Thimann & Satler, 1979a,b; Gepstein & Thimann, 1980). Second, increased insolation means more photosynthetic active radiation (PAR) which would substantially enhance trees' photosynthetic capacity and CO_2 sequestration rate until light saturation (Bonan, 2002), and result in a delayed EOS date due to the increased chlorophyll levels (He *et al*., 2005; Kim *et al*., 2008). Third, higher insolation may be resulted from more clear days (i.e., duration of sunshine). Manipulation experiments have showed that longer day length (i.e., more light duration) significantly delayed the timing of EOS (Young & Hanover, 1977; Fennell & Hoover, 1991; Fracheboud *et al*., 2009). However, photoperiod, mainly determined by a function of latitude and time of year, is not very sensitive to the climate change except under very cloudy conditions. Its effect is likely to stabilize EOS dates for a particular location. The third hypotheses may play a less important role than the first two in regulating EOS, because photoperiod alone could not explain the large interannual variation of EOS (Jeong & Medvigy, 2014). To date, the mechanisms how the insolation affect the autumn phenology remain to be further explored in the experimental efforts.

Change in EOS over the last 30 years

Considering the ensemble method mean results of the four methods (i.e., HANTS-Mr, Polyfit-Mr, double logistic, and piecewise logistic), we found a significant delay in EOS across temperate vegetation in China, with a mean rate of 0.12 ± 0.01 (mean $\pm$ SD) days per year. Similar results were reported in previous studies based on station records (Xia & Yan, 2014) or remotely sensed data (Piao *et al*., 2006; Yang *et al*., 2014). Our estimation of the trend in EOS was close to Yang *et al*. (2014) (0.13 days per year from 1982 to 2011) and Xia & Yan (2014) (0.05 days per year from 1909 to 2012), but a bit smaller than the delay amplitude (0.37 days per year from 1982 to 1999) reported by Piao *et al*. (2006). The discrepancies among them might be ascribed to differences in study period and vegetation types adopted. We found this delay across ~ 70% of our study area, but in northeastern part of Inner Mongolia, where grassland and dry climate are dominant, earlier EOS was found.

The EOS trend over temperate China could be explained by the variation in climatic factors and their correlations with EOS, but the primary climatic driving factors of the change in EOS vary among different biomes. EOS of most forests (except ENF) was positively correlated with temperature and insolation (i.e., DNF, MF, and DBF; Fig. 6, Fig. S4–7). The delayed trends of EOS were mainly driven by increases in both temperature (e.g., 0.039, 0.043 and 0.046 °C per year, respectively, by multimethods average, same in the following description, Table S1) and insolation (7.196, 2.166 and 1.577 MJ/m^2 per year, Table S1). The correlations between EOS and climatic factors (Fig. 6b, Fig. S4–7b) indicated that later EOS for the ENF was probably resulted from increased precipitation (0.169 mm per year) and temperature (0.048 °C per year). A weak correlation of EOS with insolation (Fig. 6b, Fig. S4–7b) and slightly decline in insolation during preseason (e.g., -1.330 MJ/m^2 per year, Table S1) further suggested that insolation is not a major role in the change in EOS for ENF. EOS of grasslands in Inner Mongolia (GRA-IM) was positively correlated with precipitation but negatively correlated with insolation (Fig. 6g, Fig. S4–7g). Thus, reduced precipitation (-1.340 mm per year) and increased insolation (0.722 MJ/m^2 per year) (Table S1) led to advanced EOS of grassland in these regions due to limited soil water potential. For meadows and GRA-QT on the Qinghai–Tibet Plateau, their later EOS was mainly regulated by increased temperature (e.g., 0.062 and 0.064 °C per year; Table S1). Although declined insolation and increased precipitation were also observed during preseason, the weak correlations (Fig. 6f, h, Fig. S4–7f, h) suggested that they were not the major factors. Despite our extensive efforts using multiple methods to constrain satellite-retrieved EOS, the standard deviation of EOS detected from different methods is much larger than the average trend in EOS, indicating an urgent need to further reduce the uncertainty of EOS detection. Future studies should further reduce the uncertainties by utilizing long-term filed observations to validate satellite data and finding vegetation physiology corresponding to EOS (e.g., leaf senescence), although it is still challenging due to scale mismatch between field and satellite data (e.g., Fang *et al*., 2012; Camacho *et al*., 2013; Fu *et al*., 2014a).

In summary, based on the time-series GIMMS NDVI records from 1982 to 2011 and four EOS extraction methods, we found that the EOS dates were consistently delayed in China's temperate biomes, except for dry grassland in Inner Mongolia. Furthermore, we found that, in addition to the positive role of temperature in delaying EOS, precipitation and insolation sums over the preseason also influence the phenological process in autumn, although their effect was largely biome dependent. EOS was mainly associated with temperature and insolation sum in forest biomes, except for ENF, where EOS was mainly regulated by temperature and precipitation. The impact of insolation was even stronger than that of temperature in DNF. For grassland, both temperature and precipitation modulated EOS. Precipitation regulates the timing of EOS in dry climate (e.g., GRA-IM), whereas temperature is dominant in cold regions (e.g., GRA-QT). However, other factors, such as nutrient availability (Estiarte & Peñuelas, 2015) and CO_2 concentration (Taylor *et al*., 2007; Reyes-Fox *et al*., 2014), could also modify plant phenology in autumn. Therefore, well-designed experiments are needed to better understand autumn phenology process and its response to climate change. Given the importance of autumn phenology in the study of global carbon balance, our results suggest that the effects of precipitation and insolation should be incorporated into autumn phenology models.

Acknowledgements

This study was supported by the National Basic Research Program of China (Grant No. 2013CB956303), Chinese Ministry of Environmental Protection Grant (201209031), National Natural Science Foundation of China (41125004 and 31321061), and National Youth Top-notch Talent Support Program in China. The authors also wish to thank X. Wang for helpful comments and discussions.

References

Anderegg WR, Plavcová L, Anderegg LD, Hacke UG, Berry JA, Field CB (2013) Drought's legacy: multiyear hydraulic deterioration underlies widespread aspen forest die-off and portends increased future risk. *Global Change Biology*, **19**, 1188–1196.

Balzter H, Gerard F, George C *et al.* (2007) Coupling of vegetation growing season anomalies and fire activity with hemispheric and regional-scale climate patterns in central and East Siberia. *Journal of Climate*, **20**, 3713–3729.

Biswal U, Biswal B (1984) Photocontrol of leaf senescence. *Photochemistry and Photobiology*, **39**, 875–879.

Bonan GB (2002) *Ecological Climatology: Concepts and Applications*. Cambridge University Press, Cambridge.

Borchert R, Calle Z, Strahler AH *et al.* (2015) Insolation and photoperiodic control of tree development near the equator. *New Phytologist*, **205**, 7–13.

Brandt M, Mbow C, Diouf AA, Verger A, Samimi C, Fensholt R (2015) Ground-and satellite-based evidence of the biophysical mechanisms behind the greening Sahel. *Global Change Biology*, **21**, 1610–1620.

Calle Z, Schlumpberger BO, Piedrahita L, Leftin A, Hammer SA, Tye A, Borchert R (2010) Seasonal variation in daily insolation induces synchronous bud break and flowering in the tropics. *Trees*, **24**, 865–877.

Camacho F, Cernicharo J, Lacaze R, Baret F, Weiss M (2013) GEOV1: LAI, FAPAR essential climate variables and FCOVER global time series capitalizing over existing products. Part 2: validation and intercomparison with reference products. *Remote Sensing of Environment*, **137**, 310–329.

Che M, Chen B, Innes JL *et al.* (2014) Spatial and temporal variations in the end date of the vegetation growing season throughout the Qinghai-Tibetan Plateau from 1982 to 2011. *Agricultural and Forest Meteorology*, **189**, 81–90.

Chen J, Jönsson P, Tamura M, Gu Z, Matsushita B, Eklundh L (2004) A simple method for reconstructing a high-quality NDVI time-series data set based on the Savitzky-Golay filter. *Remote Sensing of Environment*, **91**, 332–344.

Chen Y, Yang K, He J, Qin J, Shi J, Du J, He Q (2011) Improving land surface temperature modeling for dry land of China. *Journal of Geophysical Research: Atmospheres (1984–2012)*, **116**, 2156–2202.

Cleland EE, Chuine I, Menzel A, Mooney HA, Schwartz MD (2007) Shifting plant phenology in response to global change. *Trends in ecology & evolution*, **22**, 357–365.

Cong N, Piao S, Chen A *et al.* (2012) Spring vegetation green-up date in China inferred from SPOT NDVI data: a multiple model analysis. *Agricultural and Forest Meteorology*, **165**, 104–113.

Cong N, Wang T, Nan H, Ma Y, Wang X, Myneni RB, Piao S (2013) Changes in satellite-derived spring vegetation green-up date and its linkage to climate in China from 1982 to 2010: a multimethod analysis. *Global Change Biology*, **19**, 881–891.

De WitA, Su B (2005) Deriving phenological indicators from SPOT-VGT data using the HANTS algorithm. In: *2nd International SPOT-VEGETATION User Conference*, pp. 195–201. Centre National d'Etudes Spatiales, Antwerp, Belgium.

Delbart N, Kergoat L, Le Toan T, Lhermitte J, Picard G (2005) Determination of phenological dates in boreal regions using normalized difference water index. *Remote Sensing of Environment*, **97**, 26–38.

Delpierre N, Dufrêne E, Soudani K, Ulrich E, Cecchini S, Boé J, François C (2009) Modelling interannual and spatial variability of leaf senescence for three deciduous tree species in France. *Agricultural and Forest Meteorology*, **149**, 938–948.

Dreesen F, De Boeck H, Janssens I, Nijs I (2014) Do successive climate extremes weaken the resistance of plant communities? An experimental study using plant assemblages. *Biogeosciences*, **11**, 109–121.

Estiarte M, Peñuelas J (2015) Alteration of the phenology of leaf senescence and fall in winter deciduous species by climate change: effects on nutrient proficiency. *Global Change Biology*, **21**, 1005–1017.

Estrella N, Menzel A (2006) Responses of leaf colouring in four deciduous tree species to climate and weather in Germany. *Climate Research*, **32**, 253–267.

Fang H, Wei S, Liang S (2012) Validation of MODIS and CYCLOPES LAI products using global field measurement data. *Remote Sensing of Environment*, **119**, 43–54.

Fennell A, Hoover E (1991) Photoperiod influences growth, bud dormancy, and cold acclimation in Vitis labruscana and V. riparia. *Journal of the American Society for Horticultural Science*, **116**, 270–273.

Fracheboud Y, Luquez V, Björkén L, Sjödin A, Tuominen H, Jansson S (2009) The control of autumn senescence in European aspen. *Plant Physiology*, **149**, 1982–1991.

Fu YSH, Piao S, Op De Beeck M *et al.* (2014a) Recent spring phenology shifts in western Central Europe based on multiscale observations. *Global Ecology and Biogeography*, **23**, 1255–1263.

Fu YSH, Campioli M, Vitasse Y *et al.* (2014b) Variation in leaf flushing date influences autumnal senescence and next year's flushing date in two temperate tree species. *Proceedings of the National Academy of Sciences*, **111**, 7355–7360.

Gallinat AS, Primack RB, Wagner DL (2015) Autumn, the neglected season in climate change research. *Trends in Ecology & Evolution*, **30**, 169–176.

Gan S, Amasino RM (1997) Making sense of senescence (molecular genetic regulation and manipulation of leaf senescence). *Plant Physiology*, **113**, 313–319.

Garonna I, De Jong R, De Wit AJW, Mücher CA, Schmid B, Schaepman M (2014) Strong contribution of autumn phenology to changes in satellite-derived growing season length estimates across Europe (1982–2011). *Global Change Biology*, **20**, 3457–3470.

Ge Q, Wang H, Dai J (2014) Phenological response to climate change in China: a meta-analysis. *Global Change Biology*, **21**, 265–274.

Gepstein S, Thimann KV (1980) Changes in the abscisic acid content of oat leaves during senescence. *Proceedings of the National Academy of Sciences*, **77**, 2050–2053.

Günter S, Stimm B, Cabrera M *et al.* (2008) Tree phenology in montane forests of southern Ecuador can be explained by precipitation, radiation and photoperiodic control. *Journal of Tropical Ecology*, **24**, 247–258.

Guo L, Dai J, Wang M, Xu J, Luedeling E (2015) Responses of spring phenology in temperate zone trees to climate warming: a case study of apricot flowering in China. *Agricultural and Forest Meteorology*, **201**, 1–7.

Hartmann D, Klein Tank A, Rusicucci M *et al*. (2013) Observations: atmosphere and surface. In: *Climate Change 2013: The Physical Science Basis. Contribution of Working Group I to the Fifth Assessment Report of the Intergovernmental Panel on Climate Change*, pp. 159–254. Cambridge University Press, Cambridge, UK and New York, NY, USA.

He P, Osaki M, Takebe M, Shinano T, Wasaki J (2005) Endogenous hormones and expression of senescence-related genes in different senescent types of maize. *Journal of Experimental Botany*, **56**, 1117–1128.

Hilker T, Lyapustin AI, Tucker CJ *et al*. (2014) Vegetation dynamics and rainfall sensitivity of the Amazon. *Proceedings of the National Academy of Sciences*, **111**, 16041–16046.

Jakubauskas ME, Legates DR, Kastens JH (2001) Harmonic analysis of time-series AVHRR NDVI data. *Photogrammetric Engineering and Remote Sensing*, **67**, 461–470.

Jeong SJ, Medvigy D (2014) Macroscale prediction of autumn leaf coloration throughout the continental United States. *Global Ecology and Biogeography*, **23**, 1245–1254.

Jeong SJ, Ho CH, Gim HJ, Brown ME (2011) Phenology shifts at start vs. end of growing season in temperate vegetation over the Northern Hemisphere for the period 1982–2008. *Global Change Biology*, **17**, 2385–2399.

Julien Y, Sobrino J (2009) Global land surface phenology trends from GIMMS database. *International Journal of Remote Sensing*, **30**, 3495–3513.

Keskitalo J, Bergquist G, Gardeström P, Jansson S (2005) A cellular timetable of autumn senescence. *Plant Physiology*, **139**, 1635–1648.

Kim J-H, Moon YR, Wi SG, Kim J-S, Lee MH, Chung BY (2008) Differential radiation sensitivities of Arabidopsis plants at various developmental stages. In: *Photosynthesis. Energy from the Sun*, pp. 1491–1495. Springer, the Netherlands.

Menzel A, Fabian P (1999) Growing season extended in Europe. *Nature*, **397**, 659.

Miloud H, Ali G (2012) *Some Aspects of Leaf Senescence*. INTECH Open Access Publisher, Rijeka.

Moody A, Johnson DM (2001) Land-surface phenologies from AVHRR using the discrete Fourier transform. *Remote Sensing of Environment*, **75**, 305–323.

Moré JJ (1978) The Levenberg-Marquardt algorithm: implementation and theory. In: *Numerical Analysis*, pp. 105–116. Springer, Berlin.

Moulin S, Kergoat L, Viovy N, Dedieu G (1997) Global-scale assessment of vegetation phenology using NOAA/AVHRR satellite measurements. *Journal of Climate*, **10**, 1154–1170.

Munné-Bosch S, Alegre L (2004) Die and let live: leaf senescence contributes to plant survival under drought stress. *Functional Plant Biology*, **31**, 203–216.

Myneni RB, Keeling C, Tucker C, Asrar G, Nemani R (1997) Increased plant growth in the northern high latitudes from 1981 to 1991. *Nature*, **386**, 698–702.

Peng S, Piao S, Ciais P *et al*. (2013) Asymmetric effects of daytime and night-time warming on Northern Hemisphere vegetation. *Nature*, **501**, 88–92.

Philippon N, Jarlan L, Martiny N, Camberlin P, Mougin E (2007) Characterization of the interannual and intraseasonal variability of West African vegetation between 1982 and 2002 by means of NOAA AVHRR NDVI data. *Journal of Climate*, **20**, 1202–1218.

Piao S, Fang J, Zhou L, Ciais P, Zhu B (2006) Variations in satellite-derived phenology in China's temperate vegetation. *Global Change Biology*, **12**, 672–685.

Piao S, Friedlingstein P, Ciais P, Viovy N, Demarty J (2007) Growing season extension and its impact on terrestrial carbon cycle in the Northern Hemisphere over the past 2 decades. *Global Biogeochemical Cycles*, **21**. doi:10.1029/2006GB002888.

Piao S, Ciais P, Friedlingstein P *et al*. (2008) Net carbon dioxide losses of northern ecosystems in response to autumn warming. *Nature*, **451**, 49–52.

Piao S, Ciais P, Friedlingstein P, Noblet-Ducoudré ND, Cadule P, Viovy N, Wang T (2009) Spatiotemporal patterns of terrestrial carbon cycle during the 20th century. *Global Biogeochemical Cycles*, **23**. doi:10.1029/2008GB003339.

Piao S, Cui M, Chen A, Wang X, Ciais P, Liu J, Tang Y (2011) Altitude and temperature dependence of change in the spring vegetation green-up date from 1982 to 2006 in the Qinghai-Xizang Plateau. *Agricultural and Forest Meteorology*, **151**, 1599–1608.

Piao SL, Nan HJ, Huntingford C *et al*. (2014) Evidence for a weakening relationship between interannual temperature variability and northern vegetation activity. *Nature Communications*, **5**. doi:10.1038/ncomms6018.

Piao SL, Tan JG, Chen AP, Peñuelas J *et al*. (2015) Leaf onset in the northern hemisphere triggered by daytime temperature. *Nature Communications*., **6**, 6911.

Pinty B, Lavergne T, Voßbeck M *et al*. (2007) Retrieving surface parameters for climate models from Moderate Resolution Imaging Spectroradiometer (MODIS)-Multiangle Imaging Spectroradiometer (MISR) albedo products. *Journal of Geophysical Research*, **112**. doi: 10.1029/2006JD008105.

Pinzon JE, Tucker CJ (2014) A non-stationary 1981–2012 AVHRR NDVI3 g time series. *Remote Sensing*, **6**, 6929–6960.

Pinzon JE, Brown ME, Tucker CJ (2005) Satellite time series correction of orbital drift artifacts using empirical mode decomposition. In: *Hilbert-Huang Transform: Introduction and Applications*. (ed. Huang N), pp. 167–186. World Scientific Publishing Co. Pte. Ltd, Singapore.

Reyes-Fox M, Steltzer H, Trlica MJ, Mcmaster GS, Andales AA, Lecain DR, Morgan JA (2014) Elevated CO2 further lengthens growing season under warming conditions. *Nature*, **510**, 259–262.

Richardson AD, Hollinger DY, Dail DB, Lee JT, Munger JW, O'keefe J (2009) Influence of spring phenology on seasonal and annual carbon balance in two contrasting New England forests. *Tree physiology*, **29**, 321–331.

Richardson AD, Keenan TF, Migliavacca M, Ryu Y, Sonnentag O, Toomey M (2013) Climate change, phenology, and phenological control of vegetation feedbacks to the climate system. *Agricultural and Forest Meteorology*, **169**, 156–173.

Roerink G, Menenti M, Verhoef W (2000) Reconstructing cloudfree NDVI composites using Fourier analysis of time series. *International Journal of Remote Sensing*, **21**, 1911–1917.

Sakamoto T, Yokozawa M, Toritani H, Shibayama M, Ishitsuka N, Ohno H (2005) A crop phenology detection method using time-series MODIS data. *Remote Sensing of Environment*, **96**, 366–374.

Schwartz MD (2003) *Phenology: An Integrative Environmental Science*. Springer, Dordrecht.

Schwartz MD, Ahas R, Aasa A (2006) Onset of spring starting earlier across the Northern Hemisphere. *Global Change Biology*, **12**, 343–351.

Shen M, Sun Z, Wang S, Zhang G, Kong W, Chen A, Piao S (2013) No evidence of continuously advanced green-up dates in the Tibetan Plateau over the last decade. *Proceedings of the National Academy of Sciences*, **110**, E2329.

Shen M, Piao S, Cong N, Zhang G, Jassens IA (2015) Precipitation impacts on vegetation spring phenology on the Tibetan Plateau. *Global Change Biology*, **21**, 3647–3656.

Shi C, Sun G, Zhang H, Xiao B, Ze B, Zhang N, Wu N (2014) Effects of warming on chlorophyll degradation and carbohydrate accumulation of Alpine herbaceous species during plant senescence on the Tibetan Plateau. *PLoS One*, **9**, e107874.

Slayback DA, Pinzon JE, Los SO, Tucker CJ (2003) Northern hemisphere photosynthetic trends 1982–99. *Global Change Biology*, **9**, 1–15.

Sobrino JA, Julien Y, Atitar M, Nerry F (2008) NOAA-AVHRR orbital drift correction from solar zenithal angle data. *Geoscience and Remote Sensing, IEEE Transactions on*, **46**, 4014–4019.

Stöckli R, Vidale PL (2004) European plant phenology and climate as seen in a 20-year AVHRR land-surface parameter dataset. *International Journal of Remote Sensing*, **25**, 3303–3330.

Studer S, Stöckli R, Appenzeller C, Vidale P (2007) A comparative study of satellite and ground-based phenology. *International Journal of Biometeorology*, **51**, 405–414.

Tan B, Morisette JT, Wolfe RE, Gao F, Ederer GA, Nightingale J, Pedelty JA (2011) An enhanced TIMESAT algorithm for estimating vegetation phenology metrics from MODIS data. *Selected Topics in Applied Earth Observations and Remote Sensing, IEEE Journal of*, **4**, 361–371.

Taylor G, Tallis MJ, Giardina CP *et al*. (2007) Future atmospheric CO2 leads to delayed autumnal senescence. *Global Change Biology*, **14**, 264–275.

Tezara W, Mitchell V, Driscoll S, Lawlor D (1999) Water stress inhibits plant photosynthesis by decreasing coupling factor and ATP. *Nature*, **401**, 914–917.

Thimann KV, Satler S (1979a) Relation between leaf senescence and stomatal closure: senescence in light. *Proceedings of the National Academy of Sciences*, **76**, 2295–2298.

Thimann KV, Satler S (1979b) Relation between senescence and stomatal opening: senescence in darkness. *Proceedings of the National Academy of Sciences*, **76**, 2770–2773.

Tucker CJ, Slayback DA, Pinzon JE, Los SO, Myneni RB, Taylor MG (2001) Higher northern latitude normalized difference vegetation index and growing season trends from 1982 to 1999. *International Journal of Biometeorology*, **45**, 184–190.

Tucker CJ, Pinzon JE, Brown ME (2004) Global Inventory Modeling and Mapping Studies, NA94apr15b. n11–VIg, 2. 0, Global Land Cover Facility, University of Maryland, College Park, Maryland.

Tucker CJ, Pinzon JE, Brown ME *et al*. (2005) An extended AVHRR 8-km NDVI dataset compatible with MODIS and SPOT vegetation NDVI data. *International Journal of Remote Sensing*, **26**, 4485–4498.

Vermote E, Saleous NE, Kaufman Y, Dutton E (1997) Data pre-processing: stratospheric aerosol perturbing effect on the remote sensing of vegetation: correction method for the composite NDVI after the Pinatubo eruption. *Remote Sensing Reviews*, **15**, 7–21.

Visser ME, Both C (2005) Shifts in phenology due to global climate change: the need for a yardstick. *Proceedings of the Royal Society B: Biological Sciences*, **272**, 2561–2569.

Vitasse Y, Porte AJ, Kremer A, Michalet R, Delzon S (2009) Responses of canopy duration to temperature changes in four temperate tree species: relative contributions of spring and autumn leaf phenology. *Oecologia*, **161**, 187–198.

Wang X, Piao S, Xu X, Ciais P, Macbean N, Myneni RB, Li L (2015) Has the advancing onset of spring vegetation green-up slowed down or changed abruptly over the last three decades? *Global Ecology and Biogeography*, **24**, 621–631.

White MA, De Beurs KM, Didan K *et al.* (2009) Intercomparison, interpretation, and assessment of spring phenology in North America estimated from remote sensing for 1982-2006. *Global Change Biology*, **15**, 2335–2359.

Wu X, Liu H (2013) Consistent shifts in spring vegetation green-up date across temperate biomes in China, 1982-2006. *Global Change Biology*, **19**, 870–880.

Xia J, Yan Z (2014) Changes in the local growing season in Eastern China during 1909–2012. *SOLA*, **10**, 163–166.

Yang K, Koike T, Ye B (2006) Improving estimation of hourly, daily, and monthly downward shortwave radiation by importing global datasets. *Agricultural and Forest Meteorology*, **137**, 43–55.

Yang K, He J, Tang W, Qin J, Cheng CC (2010) On downward shortwave and longwave radiations over high altitude regions: observation and modeling in the Tibetan Plateau. *Agricultural and Forest Meteorology*, **150**, 38–46.

Yang Y, Guan H, Shen M, Liang W, Jiang L (2014) Changes in autumn vegetation dormancy onset date and the climate controls across temperate ecosystems in China from 1982 to 2010. *Globe Change Biology*, **21**, 652–655.

Young E, Hanover JW (1977) Effects of quality, intensity, and duration of light breaks during a long night on dormancy in blue spruce (Picea pungens Engelm.) seedlings. *Plant Physiology*, **60**, 271–273.

Yu H, Luedeling E, Xu J (2010) Winter and spring warming result in delayed spring phenology on the Tibetan Plateau. *Proceedings of the National Academy of Sciences*, **107**, 22151–22156.

Zhang X, Friedl MA, Schaaf CB *et al.* (2003) Monitoring vegetation phenology using MODIS. *Remote Sensing of Environment*, **84**, 471–475.

Zhang X, Friedl MA, Schaaf CB (2006) Global vegetation phenology from Moderate Resolution Imaging Spectroradiometer (MODIS): evaluation of global patterns and comparison with in situ measurements. *Journal of Geophysical Research: Biogeosciences 2005–2012*, **111**. doi:10.1029/2006JG000217.

Zhou L, Tucker CJ, Kaufmann RK, Slayback D, Shabanov NV, Myneni RB (2001) Variations in northern vegetation activity inferred from satellite data of vegetation index during 1981 to 1999. *Journal of Geophysical Research: Atmospheres (1984–2012)*, **106**, 20069–20083.

Zhou L, Kaufmann R, Tian Y, Myneni R, Tucker C (2003) Relation between interannual variations in satellite measures of northern forest greenness and climate between 1982 and 1999. *Journal of Geophysical Research: Atmospheres 1984–2012*, **108**, ACL 3-1–ACL 3-16. doi:10.1029/2002JD002510.

Zhu W, Tian H, Xu X, Pan Y, Chen G, Lin W (2012) Extension of the growing season due to delayed autumn over mid and high latitudes in North America during 1982–2006. *Global Ecology and Biogeography*, **21**, 260–271.

Supporting Information

Additional Supporting Information may be found in the online version of this article:

Table S1. Change in climate factors during the preseason period from 1982 to 2011.
Figure S1. Distribution of biomes in temperate China (latitude greater than 30°N).
Figure S2. Average dates and standard deviation of the end of growing season (EOS; day of year) on a biome scale in temperate China for each and all methods, i.e. HANTS-Mr, Polyfit-Mr, double logistic, piecewise logistic and their mean.
Figure S3. Preseason durations of climate factors (left panel) and frequency distributions of partial correlation coefficients between EOS and climate factors across the study area (right panel).
Figure S4. The frequency distribution of partial correlation coefficients between EOS (derived from HANTS-Mr) and climate factors for biomes distributed in temperate China.
Figure S5. The frequency distribution of partial correlation coefficients between EOS (derived from Polyfit-Mr) and climate factors for biomes distributed in temperate China.
Figure S6. The frequency distribution of partial correlation coefficients between EOS (derived from double logistic method) and climate factors for biomes distributed in temperate China.
Figure S7. The frequency distribution of partial correlation coefficients between EOS (derived from piecewise logistic method) and climate factors for biomes distributed in temperate China.